# DESIGN OF A NUMERICAL MICRO-COMBUSTOR FOR DIFFUSION FLAMES

**J. Badra* and A. Masri***
Jihad.badra@usyd.edu.au
* School of Aerospace, Mechanical and Mechatronic Engineering
The University of Sydney NSW 2006 Australia

## Abstract
This paper focuses on the development of a numerical micro-combustor capable of stabilizing a diffusion flame of methane. Different designs are tested with the objective of optimizing mixing of the methane and air streams. Stability of the flame is then ensured by increasing the temperature of the incoming streams of reactants and changing the internal conductivity of the combustor material without allowing heat transfer to the surrounding. Computations are presented for 2D and 3D versions of the micro-reactor and detailed chemical kinetics used.

It was found that the optimal design that ensures adequate mixing requires the presence of a restriction at the inlet of the combustion chamber forcing the incoming streams to converge while introducing minor pressure drop. A flame could not be sustained in an adiabatic microreactor for mixtures entering at ambient temperature (27°C) but stability was achieved at inlet temperatures of 100°C and 300°C. When heat is allowed to transfer from the products to the reactants, while keeping the microburner externally adiabatic, stronger and more stable flames were observed within the domain and the strength of the flame increases with decreasing the thermal conductivity of the walls. 3D simulations reproduced the 2D results. Such calculations provide useful information that assist in the construction of a physical micro-reactor.

## Introduction
Micro-combustion is receiving considerable attention because of the potential of constructing miniatures sources of heat or power that can be used in applications such as micro-propulsion, chemical processing and replacement for batteries in electronic devices [1, 2, 3]. Two very basic but critical outstanding issues in such devices are fluid mixing and flame stability. The latter difficulty is imposed by the small volume of the reactor and hence the flame's proximity to solid surfaces resulting in significant quenching due to losses of heat as well as important reactive radicals. Mixing is limited by the narrow channels, the low velocities and hence the laminar flows that result only in molecular mixing of species. Another added difficulty, albeit less serious, is the development of micro-fabrication techniques that can produce complex components at the scale required for the micro-combustor [1, 2, 4, 5].

This paper temporarily by-passes the issue of micro-fabrication by dealing only with a numerical micro-combustor. It deals however, with the former two issues of mixing and flame stability and presents a somewhat novel design of a micro-combustor for diffusion flames where mixing of the separated fuel and air streams is optimized such as stoichiometric mixtures are formed. Flame stability is ensured by manipulating the heat loss to the reactor through a judicious choice of conductivities as well as feedback heat transfer from the combustion products. It is believed that the issues learnt from such design and optimization will be important in enabling the construction of a workable prototype combustor.

Enhancing mixing in micro-fluidic devices has received considerable attention with the use of passive or static micro-mixer to increases the surface area in contact between the mixing fluids [6]. Two types of passive mixers were used: the T-mixer [7] and the Y-mixer [8]. The fluids enter the mixer side by side in a parallel fashion. The entering steams are split into sub-streams and woven together [9, 10]. Another method of enhancing mixing is through injecting both fluids into each other as a counter-flow to cause fragmentation of the streams [11]. Other techniques used to increase chaotic advection include: (i) irregularly shaped walls to provide obstacles to the flow, (ii) the addition of obstacles in the channel [12, 13]; and (iii) zig-zag shaped channels [14]. For flows with low Reynolds numbers in the range 1 to 100, [15, 16] Herringbone style grooves in the walls can be used.

Earlier efforts to construct micro-combustors have been largely limited to premixed flames to by-pass issues of mixing and focus on the combustion stability [17, 18, 19]. An exception to this is the work of Shannon et al. [20, 21] who investigated the mixing (albeit not optimized) and stability of diffusion flames in a range of micro-combustors. Other key features of the work of Shannon et al, [20] lie in using different materials for the combustors, and in the treatment of the surface to minimize the quenching of radicals. It is worth noting that these studies do not use a surface catalyst so that combustion is largely dictated by the homogeneous phase.

This paper presents numerical designs of micro-burners for diffusion flames where the mixing of fuel and oxidant is gradually optimized. The issue of flame stability and its sensitivity to heat losses even within the burner is addressed by selectively varying the conductivity of the solid material. While the parametric studies are performed in 2D, a 3D version of the burner is also computed. The present calculations are restricted to a burner assembly that is adiabatic although heat transfer within the burner is accounted for.

**Numerical Set up**

The commercial Fluent 12 [22] CFD package is used for all calculations presented here. The Tri-pave meshing scheme is adopted allowing us to control the aspect ratio and refine the mesh where needed. The computed species concentrations as well as temperature profiles at various locations in the domain are compared for various grid sizes to ensure that that a grid-independent solution is presented. The flow, reactants and energy equations are solved first so as to provide a good starting point for the more complicated case where gaseous reactions dominate the solution. The results presented in this paper are obtained from the non-iterative time advancement unsteady state part of the solver for a time step of 1 μs and then the steady laminar solver is turned on to ensure the solution is fully converged. A second order discretization scheme has been utilized for all the equations solved and the under relaxation parameters have been modified slightly to help converge and stabilize the solution.

The Smooke [23] mechanism with the corresponding thermodynamic database file is used for the volumetric reactions. The GRI2.11 transport database file is used with the selected mechanisms to account for chemical reactions with mass, heat and thermal conductivity diffusivity. Since the flow is laminar, the full multi-component diffusion model has to be enabled for the careful treatment of chemical species diffusion in the species transport and energy equations. Thermal diffusion is solved as well and detailed gas chemistry is implemented using the ISAT algorithm where the ISAT error tolerance of 1e-6 was used.

**Mixing Issues**

In order to understand the mixing mechanism of fluids in micro-combustors, it is better to examine the conservation equations of momentum, energy and species normalised by the characteristic length and parameters of the device [1], shown below.

$$\frac{l_c}{t_c u_c}\frac{\partial \bar{u}}{\partial \bar{t}} + \bar{u}\frac{\partial \bar{u}}{\partial \bar{x}} = -\frac{p_c}{\rho_c u_c^2}\frac{1}{\bar{\rho}}\frac{\partial \bar{p}}{\partial \bar{x}} + \frac{1}{Re}\bar{\nu}\frac{\partial^2 \bar{u}}{\partial \overline{x^2}} + \frac{g l_c}{u_c^2} \quad (1)$$

$$\frac{l_c}{t_c u_c}\frac{\partial \bar{T}}{\partial \bar{t}} + \bar{u}\frac{\partial \bar{T}}{\partial \bar{x}} = \frac{1}{Pe}\bar{\alpha}\frac{\partial^2 \bar{T}}{\partial \overline{x^2}} + Da\frac{Q}{\bar{C}_{pT_c}}\bar{\dot{w}}'' \quad (2)$$

$$\frac{l_c}{t_c u_c}\frac{\partial \bar{y}_i}{\partial \bar{t}} + \bar{u}\frac{\partial \bar{y}_i}{\partial \bar{x}} = \frac{1}{LePe}\bar{D}\frac{\partial^2 \bar{y}_i}{\partial \overline{x^2}} + Da\frac{1}{y_{ic}}\bar{\dot{w}}'' \quad (3)$$

The above equations are derived in the assumption of a continuum fluid. They contain a number of dimensionless numbers, noticeably the Reynolds number Re, the Péclet number Pe, the Damköhler number Da and the Lewis number Le. The Péclet number Pe is defined as the ratio of the rate of advection of the flow to the rate of diffusion can be described by the equation below.

$$Pe = \frac{l_c u_c}{\alpha_c} \quad (4)$$

The Damköhler number Da is defined as characteristic mixing time or the ratio of time it takes a fluid to travel a certain characteristic distance to the time it takes for the chemical reaction to complete, which is defined by the equation below.

$$Da = \frac{\dot{w}_c'' l_c}{\rho_c u_c} \quad (5)$$

The Lewis number Le is defined as the ratio of thermal diffusivity to mass diffusivity, with the equation shown below.

$$Le = \frac{\alpha_c}{D_c} \quad (6)$$

For analysing the mixing mechanism, it is more important to examine the values for Reynolds and Péclet numbers since they are the terms that affects the diffusion terms and because there is no difference in temperature between the two streams of fuel and oxidizer.

In the common mixing systems, the characteristic length of the components is large, and generally the Reynolds and Péclet numbers are also large. The flow is therefore turbulent. Looking at Equations (1), (2) and (3), the diffusive terms are multiplied by the inverse of Reynolds number in equation (1) and the inverse of Péclet number in equation (2) and (3). Therefore, in the case of a large mixing system, viscous and diffusive terms are small relative to advection terms. As the characteristic lengths of the components become smaller (such is the case with microburners), the values of Reynolds and Péclet numbers decrease since the flow laminarizes and the advection terms become negligible. Mixing in such small devices is harder to achieve since it is largely driven by molecular processes so that a judicious design of the mixing streams is needed. The next section presents results for two micro-burner designs: the first leads to inadequate mixing while the second is an almost perfect mixer.

Micro-burner I: inadequate mixing

In this burner, shown in Fig.1, a number of curved baffles are used to break each of the fuel and air streams into a number of sub-streams that are gradually guided at an angle into the mixing chamber. Pure methane is fed from the left inlet of the microburner and pure air (21% Oxygen and 79% Nitrogen) is entering from the right inlet. Both stream of methane and air are at ambient temperature (27°C) and enter with a mean velocity of 0.5 m/s. As can be seen

from the false color contours of methane shown in Fig. 1, the two streams have not mixed properly and almost pure methane and pure oxygen are still seen separately on either side of the middle of the chamber. Given the equal amounts of fuel and air injected here, perfect mixing corresponds to a uniform mass fraction of methane=0.05. It is evident that this is only obtained in a small strip to the right side of the chamber. Of particular note here is the fact that the guiding baffles are doing little to aid the mixing process

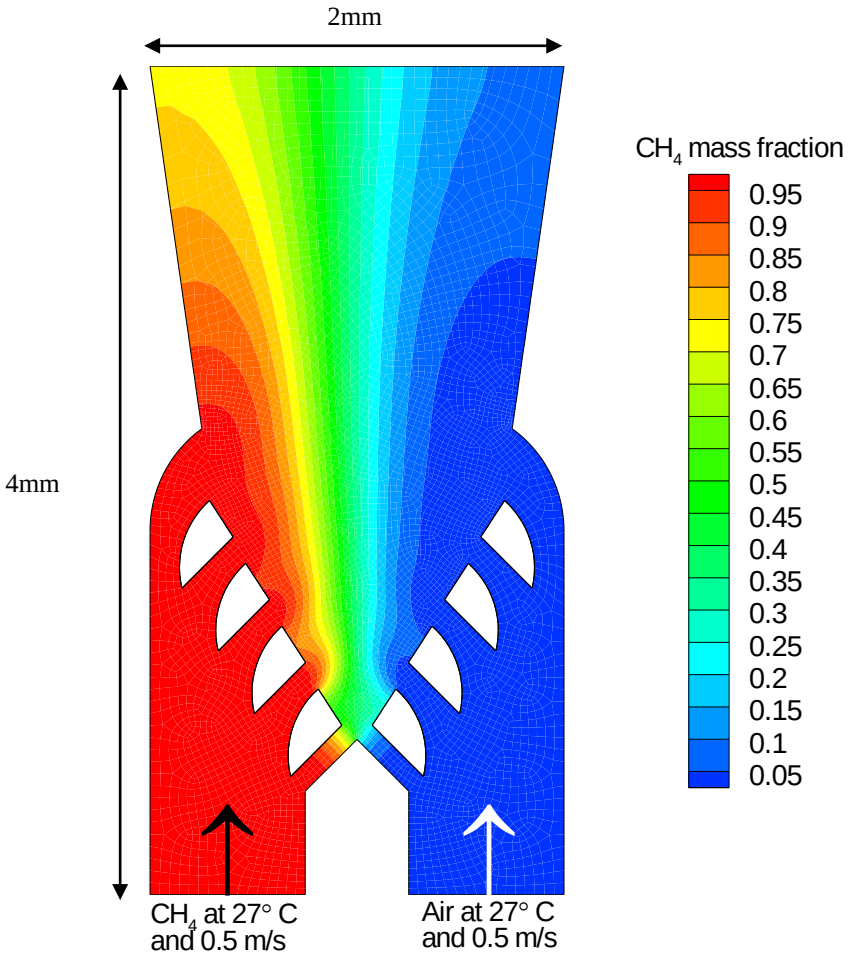


**Figure 1**. Contours of methane mass fraction in a micro-burner I.

Micro-burner II: adequate mixing

A schematic of micro-burner II (Fig. 2) shows overall dimensions of 2.5 by 4.6mm with a fuel inlet channel, 0.08mm wide next to a larger air inlet channel, 0.75mmwide. Mixing of fuel and air occurs on impact and is almost complete before the mixture reaches the restriction as clearly evident from the false color contours shown on Fig. 2. The narrowest passage at the restriction is 0.1mm. It is worth noting here that the introduction of this narrow inlet to the combustion chamber is an important feature of this design. It allows the upstream fuel and air stream to converge and mix prior to entering the reactor. The disadvantage of this restriction lies in the pressure drop that it introduces although it has been shown earlier that is minor and corresponds to only 50 Pascals. The triangular combustion chamber downstream of the restriction allows for the gas expansion with its widest point at the downstream end of the burner leading to two side channels for the exhaust. These exhaust channels wrap around the body of the burner and the inlet streams leading to some pre-heating of the incoming gases.

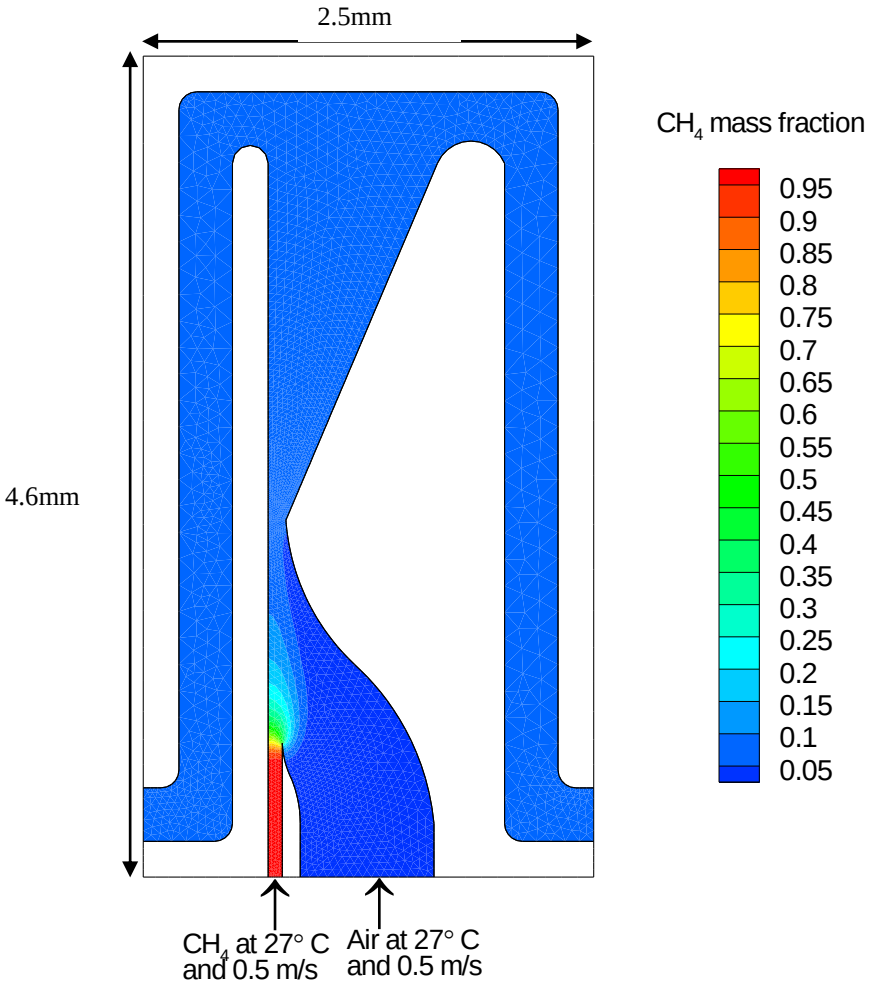


**Figure 2**. Contours of methane mass fraction in micro-burner II.

For the two-dimensional burner configuration shown in Fig. 2, the volume flow-rate of air is 9.375 times that of methane leading to an overall stoichiometric composition. This is achieved just before the restriction inlet so that a mixture with Ø≈1 enters the combustion chamber. Note that both streams of fuel and air have the same velocity of 0.5m/s at 27$^{o}$C.The light blue color in Fig. 2 refers to a stoichiometric mass fraction of methane of ~0.053 filling the remainder of the chamber implying perfect mixing conditions. This burner design (or minor variation thereof) is used here for all subsequent calculations and is later extended to a three-dimensional configuration

**Combustion in 2D micro-burner II**

In this section, solutions are presented for three reacting cases with the following conditions: (i) an adiabatic, non-conductive burner with inlet streams at 27$^{o}$C leading to an extinguishing flame, (ii) an adiabatic, non-conductive burner with inlet streams at 100$^{o}$C and 300$^{o}$C leading to a stable flame, and (iii) an adiabatic burner with internal conduction and inlet streams at 300$^{o}$C leading to a stable flame. In this latter case, the outer boundaries of the burner are adiabatic but the inner elements are conductive enabling heating of the inner channels.

Extinguishing case: adiabatic, non-conductive with inlet at 27$^{o}$C

A sequence of false color contours of the computed temperature are shown in Fig. 3 at various times after ignition for the case where both methane and air streams enter the burner at a velocity of 0.5m/s and a temperature of 27$^{o}$C. First a solution for the non-reacting case is

obtained showing almost complete mixing before the restirciton as shown in Fig. 2. This non-reacting solution shown in Fig. 2 is used a starting point for the reacting case and gnition is initiated by introducing in the first iteration a hot patch that has a temprature of 2500K and dimensions of 0.66mm x 0.85mm centred in the middle of the triangular combustion chamber downstream of the restriction. The case considered here is fully adiabatic.

It is evident from the sequence shown in Fig. 3 that the flame cannot be sustained for these inlet conditions and extinguishes with the initial combustion products washing off through the left and right outlets. It can be seen from the images at 100 μs that the flame which is initiated at the hot spot and propagates back to consume the unburnt mixture of methane and air. The flame extinguishes as indicated by the decreased peak temperature and the combustion products gradually start to flush out of the combustion chamber through the side outlets as shown from the contours of the 1 to 6ms. The combustion products continue to be flushed out until the fully non-reacted solution is recovered at times > 8ms.

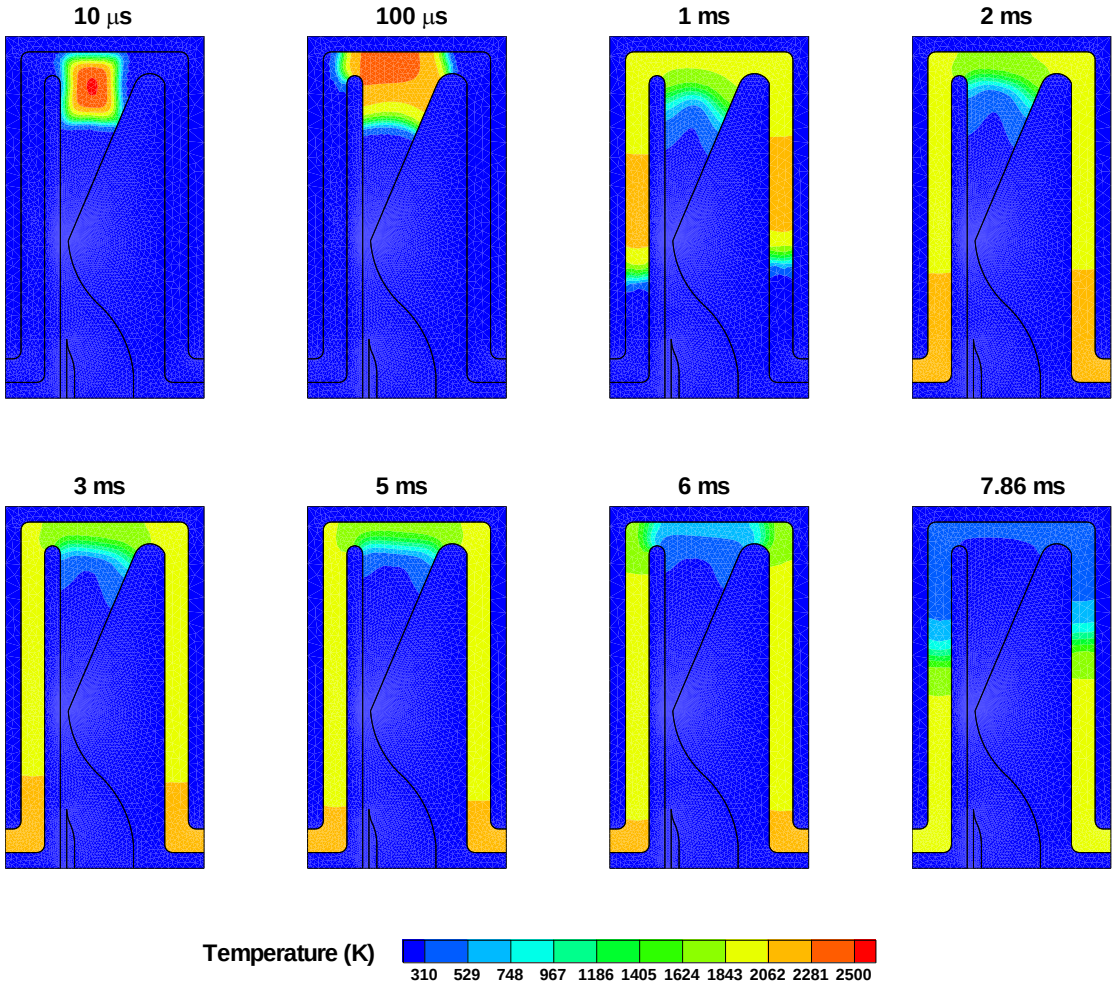


**Figure 3**. Time history of the flame for $T_{jet}$ =27°C and adiabatic microburner.

Burning case: adiabatic, non-conductive with inlet at 100°C and 300°C

Given that the previous case extinguished, the inlet mixture temperature is increased here from 27°C to 100°C and 300°C for the same adiabatic case to ensure that a stable flame is indeed obtained. The computed steady state temperature and selected species mass fractions (OH, $O_2$ and CO) for the steady-state case are shown in Fig. 4. Note that for the temperature plots, the solid sections of the burner (which are assumed here to have zero conductivity) are

shown to be at the same temperatures of the entering mixture since no heat transfer is allowed. It is evident from these results that, as the temperature of the incoming mixture increases, the peak mass fraction of OH increases and the flame front moves upstream closer to the restriction. This is consistent with the corresponding increase in flame speed at the hotter conditions. Oxygen is fully consumed in both cases and CO forms right on the reaction zone and gets consumed quickly to form $CO_2$ (not shown here) which exists in higher quantities for the hotter inlets as a result of stronger reaction zone.

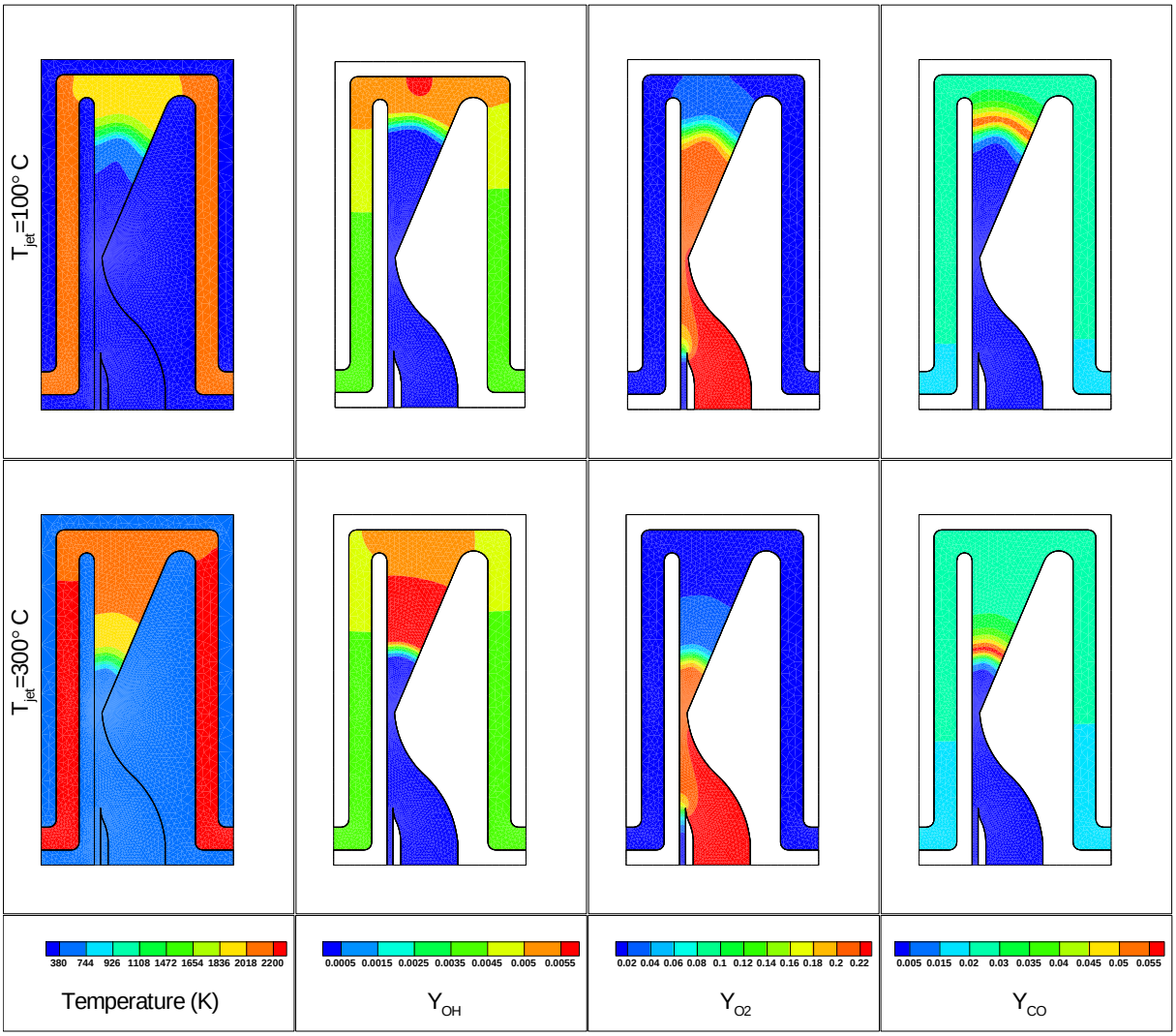


**Figure 4**. Contours of temperature, mass fraction of OH, O2 and CO for adiabatic microburner at different jet temperatures.

Burning case: adiabatic with internal heat conduction and inlet at 300$^{o}$C

This section enables some heat conduction within the inner core of the burner but no heat external heat losses so that the overall burner remains adiabatic. Properties of a range of materials are simulated here ranging from aluminum to fused silica as shown in Table 1. When the temperature of the mixture is 27$^{o}$C, the flame is extinguished so calculations are shown here for cases where the temperature of the mixture is fixed at 300$^{o}$C.

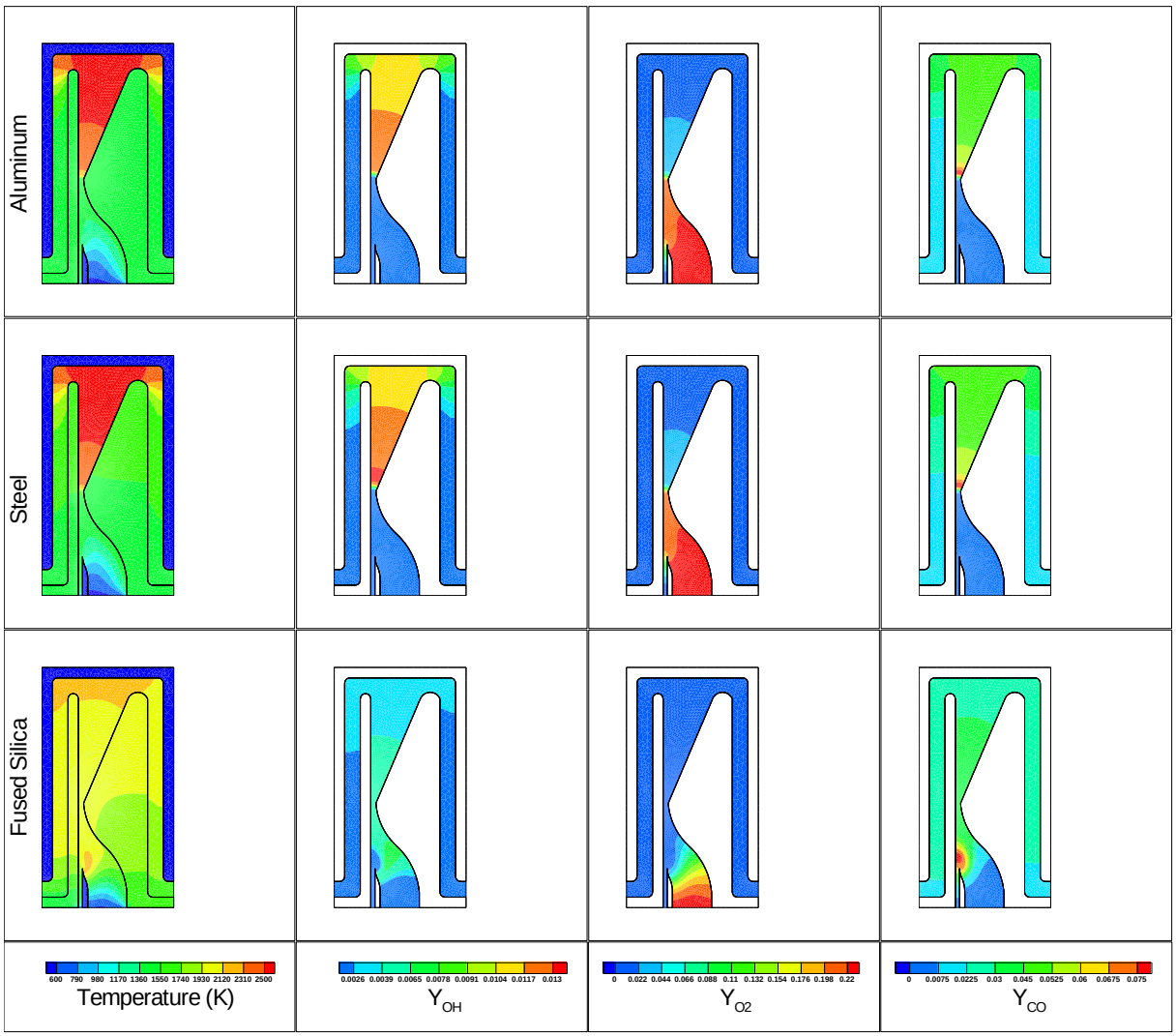


**Figure 5**. Contours of temperature, mass fraction of OH, O2 and CO for an adiabatic but internally conductive microburner using different materials.

**Table 1.** Material properties as adopted in the current calculations.

| Material | Density (kg/m$^3$) | Specific heat (Cp) (J/kg.K) | Thermal conductivity (w/m.K) |
|---|---|---|---|
| Aluminum | 2719 | 871 | 202.4 |
| Steel | 8030 | 502.48 | 16.27 |
| Fused silica | 2203 | 740 | 1.3 |

Figure 5 shows the computed contours of temperature and selected species mass fractions (OH, $O_2$ and CO) for three cases where the material properties within the core of the burner change from aluminum to steel to fused silica. It is clear that the flame stability, as marked by the peak temperature and the maximum levels of OH formed, improves with the decreasing conductivity of the material. With fused silica, which has a low conductivity of 1.3w/m.K, the flame front has actually moved upstream of the neck of the combustion chamber and some reaction has occurred at the tip of the splitter plate separating the fuel and air streams where the temperature is 2100K and some CO as well as OH have formed. Aluminum and steel are very similar in terms of flame temperature and its composition but both are significantly different than fused silica. When using fused silica, the flame gets hotter in the initial stages

and peak temperatures of 2700K are observed at the restriction, the flame passes the neck and starts burning on top of the splitter as shown in Fig. 5, where richer methane/air mixtures exist (see Fig. 2). This explains the lower flame temperature when using fused silica compared to aluminum and steel, where the flame sits at the neck and burn almost stoichiometric methane/air mixtures.

**Combustion in 3D micro-burner II**

The 3D version of micro-burner II is slightly modified from its 2D version, where the products travel closer to reactants for longer time to allow better heat exchange between hot products and reactants. The micro-reactor is sandwiched between two solid plates that are 1mm apart from each other. Only half of the domain is modeled due to symmetry along the 3$^{rd}$ dimension and the domain is meshed using 85,000 triangular cells and ran for mixing only and the results for mixing were the same as in 2D. Figure 6 shows the temperature contours for a case, where the inlet temperatures of fuel and air are set to $T_{jet}$=100°C, the velocities of both stream are 0.5m/s and the material that allows internal heat transfer is aluminum. Overall, the burner is adiabatic so that no external heat losses are allowed.

As can be observed from the computed temperature contours shown in Fig. 6, the flame is stable and the reaction zone sits close to the restriction. The internal heat exchange with the combustion products has allowed the entering reactants to heat even further reaching a temperature of 1400K. Further investigation on the 3D microburner will be carried out in later work with the inclusion of a catalyst to assist ignition and stabilize the flame inside the burner.

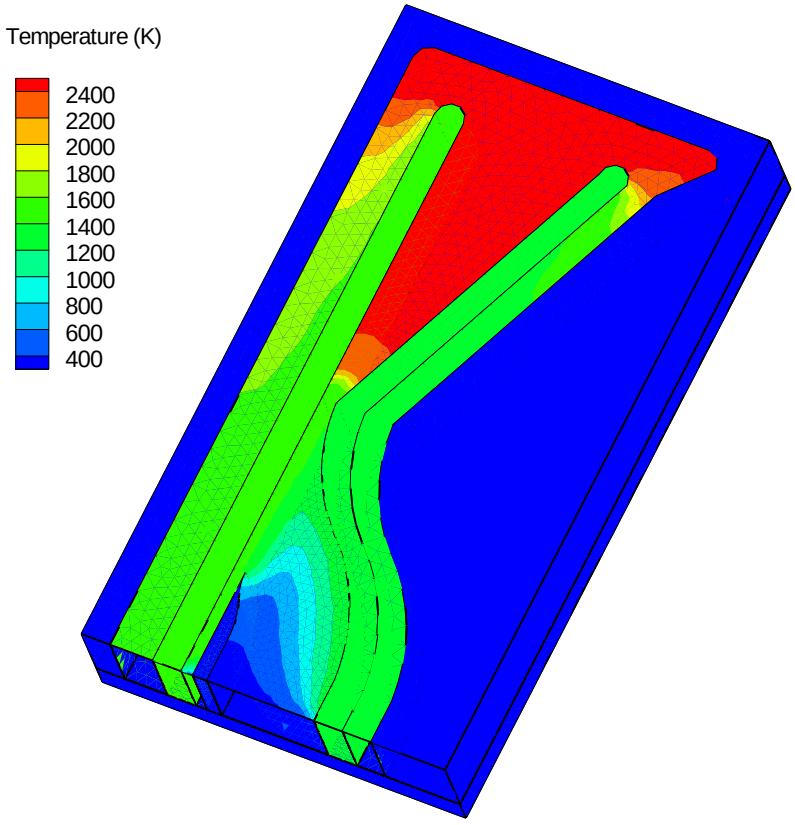


**Figure 6.** 3D Temperature contours for $T_{jet}$=100°C and using aluminum as the conductive material.

## Conclusions

This paper presents a numerical design of a microreactor that mixes separate fuel and air streams and stabilizes a diffusion flame. An optimum design has been achieved to perfectly mix the fuel and air to stoichiometric mixtures before entering the combustion chamber. Flame stabilization inside the microburner is performed using both 2D and 3D geometries. It was found that for totally adiabatic microburner a flame could only be sustained if the incoming gases are heated to at least 100°C and as the mixture temperature increases the flame moves upstream because of the increased laminar flame speed. When heat transfer is allowed within the reactor, without allowing heat transfer to the surroundings, the flame becomes more stable and stabilized further upstream within the combustion chamber. Further decreasing the thermal conductivity results is a flame traveling beyond the neck and sitting on top of the splitter. 3D simulations back up the 2D calculations for the externally adiabatic cases and further studies on 3D will be explored in later work.

## Nomenclature

| | |
|---|---|
| $\bar{C}_p$ | normalized specific heat, $\bar{C}_p = C_p/C_{pc}$ |
| $C_p$ | specific heat |
| $C_{pc}$ | characteristic specific heat |
| $\overline{D}$ | normalized diffusion coefficient, $\overline{D} = D/D_C$ |
| $D$ | diffusion coefficient |
| $Da$ | Damköhler number, $Da = \dot{w}_c^{''} l_c/\rho_c u_c$ |
| $D_C$ | characteristic diffusion coefficient |
| $g$ | gravity |
| $Le$ | Lewis number, $Le = \alpha_c/D_c$ |
| $l_c$ | characteristic length of the device |
| $Pe$ | Péclet number, $Pe = l_c u_c/\alpha_c$ |
| $p_c$ | characteristic pressure |
| $Q$ | heat rate |
| $Re$ | Reynolds number, $Re = u_c l_c/\nu_c$ |
| $t$ | time |
| $\bar{t}$ | normalized time, $\bar{t} = t/t_c$ |
| $t_c$ | characteristic time |
| $T$ | temperature |
| $\bar{T}$ | normalized temperature, $\bar{T} = T/T_c$ |
| $T_c$ | characteristic temperature |
| $u$ | velocity |
| $\bar{u}$ | normalized velocity, $\bar{u} = u/u_c$ |
| $u_c$ | characteristic velocity |
| $\dot{w}''$ | reaction rate |
| $\bar{\dot{w}}''$ | normalized reaction rate, $\bar{\dot{w}}'' = \dot{w}''/\dot{w}_c^{''}$ |
| $\dot{w}_c^{''}$ | characteristic reaction rate |
| $x$ | spatial coordinate |
| $\bar{x}$ | normalized spatial coordinate, $\bar{x} = x/x_c$ |
| $x_c$ | characteristic spatial coordinate |
| $y_i$ | mass fraction of species *i* |
| $\bar{y}_i$ | normalized mass fraction of species *i*, $\bar{y}_i = y_i/y_{ic}$ |
| $y_{ic}$ | characteristic mass fraction of species *i* |
| $\alpha$ | thermal diffusivity |
| $\bar{\alpha}$ | normalized thermal diffusivity, $\bar{\alpha} = \alpha/\alpha_c$ |

$\alpha_c$ characteristic thermal diffusivity
$\rho_c$ characteristic density
$\nu$ kinematic viscosity
$\bar{\nu}$ normalized kinematic viscosity, $\bar{\nu} = \nu/\nu_c$
$\nu_c$ characteristic kinematic viscosity

Subscripts
*c* characteristic value
*i* species *i*

Superscripts
_ normalized variable with its characteristic value
. rate

**Acknowledgment**
This research is supported by the Australian Research Council

**References**
[1] Fernandez-Pello, A. C., "Micropower Generation Using Combustion: Issues and Approaches", *Proceedings of the Combustion Institute*. 29: 883-899 (2002).
[2] Chao, Y. C. Chen, G. B. Hsu, C. J. Leu, T. S. Wu, C. Y., "Operational Characteristics of Catalytic Combustion in a Platinum Microtube", Combust. Sci. and Tech. 176: 1755-1777 (2004).
[3] Smyth, S. A. Christensen, K. T. Kyritsis, D. C., "Intermediate Reynolds number flat plate boundary layer flows over catalytic surfaces for "micro"-combustion applications", Proceedings of the Combustion Institute. 32: 3035-3042 (2009).
[4] Vican, J., Gajdeczko, B., F., Dryer, F., L., Milius, D., L., Aksay, I., A., Yetter, R., A., "Development of a micoreactor as a thermal source for microelectromechanical systems power generation", *Proceedings of the Combustion Institute*. 29: 909-916 (2002).
[5] Peterson, R. B. Hatfield, J. M., "A Catalytically Sustained Microcombustor Burning Propane", *Proceedings of the 2001 International Mechanical Engineering Congress and Exposition (IMECE)*, American Society of Civil Engineers. New York, (2001)..
[6] Hessel, V., Lowe, H., Schonfeld, F., "Micomixers – a review on passive and active mixing principles", *Chemical Engineering Science*. 60: 2479-2501 (2005).
[7] Jen, C., P., Wu, C., Y., Lin, Y., C., "Design and simulation of the micromixer with chaotic advection in twisted microchannels", *Lab Chip*. 3: 77-81 (2003).
[8] Gobby, D., Angeli, P., Gavriilidis, A., "Mixing characteristics of T-type microfuidic mixers", *Journal of Micromechanics and Microengineering*. 11: 126-132 (2001).
[9] Hardt, S., Schonfeld, F., "Laminar mixing in different interdigital micromixers: II. Numerical simulations", *Aiche Journal*. 49: 578-584 (2003).
[10] Schonfeld, F., Hessel, V., Hofmann, C., "An optimised split-and-recombine micro-mixer with uniform 'chaotic' mixing", *Lab Chip*. 4: 65-69 (2004).
[11] Drese, K., S., "Optimisation of interdigital micromixers via analytical modeling-exemplified with the SuperFocus mixer", *Chemical Engineering Journal*. 101: 403-407 (2004).
[12] Norton, D., G., Wetzel, E., D., Vlachos, D., G., "Fabrication of single-channel catalytic microburners: Effect of confinement on the oxidation of hydrogen/air mixtures", *Industrial & Engineering Chemistry Research*. 43: 4833-4840 (2004).

[13] Losey, M., W., Jackman, R., J., Firebaugh, S., L., Schmidt, M., A., Jensen, K., F., "Design and fabrication of microfuidic devices for multiphase mixing and reaction", J. Microelectromech. Syst. 11: 709-717 (2002).
[14] Ehrfeld, W., Golbig, K., Hessel, V., Lowe, V., Richter, T., "Characterization of mixing in micromixers by a test reaction: Single mixing units and mixer arrays", *Industrial & Engineering Chemistry Research.* 38: 1075-1082 (1999).
[15] Stroock, A., D., Dertinger, S., K., W., Ajdari, A., Mezic, I., Stone, H., A., Whitesides, G., M., "Chaotic mixer for microchannels", *Science*. 295: 647-651 (2002).
[16] Kee, S., P., Gavriilidis, A., "Design and characterization of the staggered herringbone mixer", *Chemical Engineering Journal*. 142: 109-121 (2008).
[17] Appel, C., Mantzaras, J., Schaeren, R., Bombach, R., Inauen, A., Kaeppeli, B., Hemmerling, B., stampanoni, A., „An Experimental and Numerical Investigation of Homogeneous Ignition in Catalytically Stabilized Combustion of Hydrogen/Air Mixtures Over Platinum", *Combustion and Flame*. 128: 340-368 (2002).
[18] Reinke, M., Mantzaras, J., Schaeren, R., Bombarch, R., Inauen, A., Schenker, S., "Homogeneous ignition of CH4/air and H2O and CO2-diluted CH4/O2 mixtures over Pt; an experimental and numerical investigation at pressures up to 16 bar", *Proc. Combust. Inst*. 30: 2519-2527 (2005).
[19] Dogwiller, U., Benz, P., Mantzaras, J., "Two-Dimensional Modelling for Catalytically Stabilized Combustion of a Lean Methane-Air Mixture With Elementary Homogeneous and Heterogeneous Chemical Reactions", *Combustion and Flame*. 116: 243-258 (1999).
[20] Meisse, C. M. Masel, R. I. Jensen, C. D. Shannon, M. A. Short, M., "Submillimetre-Scale Combustion", *American Institute of Chemical Engineers Journal*. 50: 3206-3214 (2004).
[21] Miesse, C., Masel, R., I., Short, M., Shannon, M., A., "Experimental Observations of Methane-Oxygen Diffusion Flame in a Sub-millimeter Microburner", *Combustion Theory and Modelling*. 9: 77-92 (2005).
[22] FLUENT 12, ANSYS, http://www.ansys.com/Products/Simulation+Technology/Fluid+Dynamics/ANSYS+FLUENT, 2009, USA.
[23] Smooke, M., D., Puri, I., K., Seshadri, K., "A comparison Between Numerical Calculations and Experimental Measurements of the Structure of a Counterflow Diffusion Flame Burning Diluted Methane in Diluted Air", The Combustion Institute. 21: 1783-1792 (1986).